3D finite-difference transient electromagnetic modeling with a whole-space initial field

Abstract: A three-dimensional finite-difference time-domain transient electromagnetic forward modeling method with whole-space initial field is proposed to improve forward efficiency and flexibility. The open-source software WFTEM3D is developed based on this method with two language versions: a FORTRAN code and a MATLAB code. First the scheme calculates the whole-space initial field excited by magnetic dipole sources at an initial time after the current is switched off. Then the scheme steps Maxwell's equations in time using a staggered grid and a modified DuFort-Frankel method. Multiple magnetic dipole sources are superimposed to achieve the modeling for large loop configurations. The air is included into the grids and the Dirichlet boundary condition is used on the outer boundaries. The forward modeling method has three advantages. First, the method can be used to simulate both the whole-space model and the half-space model. Second, big mesh growth factors of 1.5–3 are allowed, which significantly improves the computational efficiency and facilitates the simulation of the multi-scale model. Third, the approximate initial field can be calculated using a conductivity independent of the model, which facilitates the simulation of the non-flat topography model. These advantages are tested by examples. The model of a conductive brick in a half-space and the model of a complex conductor at a vertical contact are simulated. The run-times are 0.48 and 9.72 s, respectively, on an ordinary computer with Intel Core i7-6700 CPU, and the solutions are consistent with that presented in the literature. Examples of a multi-scale model with three conductive bricks, a valley model, and a hill model are simulated, which further verify these advantages.

METHOD

Governing equations

Maxwell's equations in source-free media are as follows:

$$\begin{cases} \nabla \times \boldsymbol{E} = -\dfrac{\partial \boldsymbol{B}}{\partial t} & (a) \\ \nabla \times \boldsymbol{H} = \varepsilon \dfrac{\partial \boldsymbol{E}}{\partial t} + \sigma \boldsymbol{E} & (b) \\ \nabla \cdot \boldsymbol{E} = 0 & (c) \\ \nabla \cdot \boldsymbol{H} = 0 & (d) \end{cases}, \tag{1}$$

where $\boldsymbol{E}$ is electromagnetic intensity, $\boldsymbol{B}$ is magnetic induction intensity, $\boldsymbol{H}$ is magnetic field intensity, σ is conductivity, ε is dielectric constant, t is time, $\boldsymbol{B} = \mu \boldsymbol{H}$, and μ is permeability.

The displacement current term $\varepsilon \dfrac{\partial \boldsymbol{E}}{\partial t}$ is negligible and can be removed in transient electromagnetic methods. In order to construct an explicit scheme, an artificial displacement current term $\gamma \dfrac{\partial \boldsymbol{E}}{\partial t}$ is introduced using the modified DuFort-Frankel method (Wang and Hohmann, 1993):

$$\begin{cases} \nabla \times \boldsymbol{E} = -\dfrac{\partial \boldsymbol{B}}{\partial t} & (a) \\ \nabla \times \boldsymbol{H} = \gamma \dfrac{\partial \boldsymbol{E}}{\partial t} + \sigma \boldsymbol{E} & (b) \\ \nabla \cdot \boldsymbol{E} = 0 & (c) \\ \nabla \cdot \boldsymbol{H} = 0 & (d) \end{cases}. \tag{2}$$

Equations 2a and 2b in the Cartesian coordinate system are as follows:

$$\frac{\partial E_z}{\partial y} - \frac{\partial E_y}{\partial z} = -\mu \frac{\partial H_x}{\partial t}, \tag{3}$$

$$\frac{\partial E_x}{\partial z} - \frac{\partial E_z}{\partial x} = -\mu \frac{\partial H_y}{\partial t}, \tag{4}$$

$$\frac{\partial E_y}{\partial x} - \frac{\partial E_x}{\partial y} = -\mu \frac{\partial H_z}{\partial t}, \tag{5}$$

$$\frac{\partial H_z}{\partial y} - \frac{\partial H_y}{\partial z} = \gamma \frac{\partial E_x}{\partial t} + \sigma E_x, \tag{6}$$

$$\frac{\partial H_x}{\partial z} - \frac{\partial H_z}{\partial x} = \gamma \frac{\partial E_y}{\partial t} + \sigma E_y, \tag{7}$$

$$\frac{\partial H_y}{\partial x} - \frac{\partial H_x}{\partial y} = \gamma \frac{\partial E_z}{\partial t} + \sigma E_z. \tag{8}$$

Considering the non-divergence characteristic of the magnetic field (equation 2d), H_z is calculated by H_x and H_y (Wang and Hohmann, 1993), and equation 5 is replaced by

$$\frac{\partial H_x}{\partial x} + \frac{\partial H_y}{\partial y} = -\frac{\partial H_z}{\partial z}. \tag{9}$$

Equations 3, 4 and 6-9 constitute the compute equations of transient electromagnetic field in source-free media.

Model discretization and time stepping

The model is discretized into a number of cells as shown in Figure 1a. As Figure 1b shows, a staggered grid (Yee, 1966) is used to define the electric and magnetic fields. The electric field is sampled at the centers of the edges, and the magnetic field is sampled at the centers of the faces.

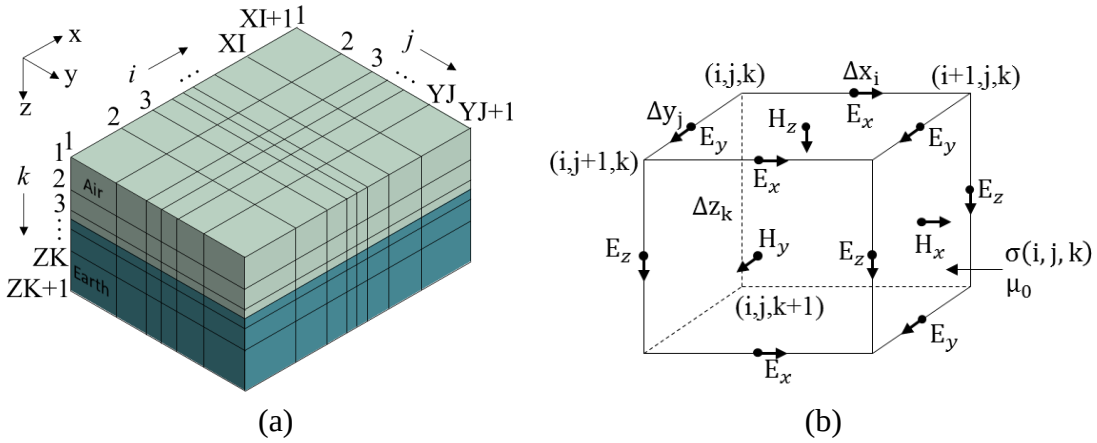

(a) (b)

Figure 1. Model discretization and a staggered grid.

First we calculate $\boldsymbol{E}$ at t_0 and $\boldsymbol{H}$ at $t_0 + \Delta t_0/2$ using equation 25. Then we step Maxwell's equations in time; with $\boldsymbol{E}$ at t_n and $\boldsymbol{H}$ at $t_n + \Delta t_n/2$, we extrapolate $\boldsymbol{E}$ to t_{n+1} using equations 6-8; then with $\boldsymbol{H}$ at $t_n + \Delta t_n/2$ and $\boldsymbol{E}$ at t_{n+1}, we extrapolate $\boldsymbol{H}$ to $t_{n+1} + \Delta t_{n+1}/2$ using equations 3, 4 and 9, and so on.

Finite-difference equations

We use $f(x, y, z, t)$ to represent field component, and the discretization form is written as

$$f(x, y, z, t) = f(i\Delta x, j\Delta y, k\Delta z, n\Delta t) = f^n(i, j, k). \tag{10}$$

The central difference of the space and time derivative of $f(x, y, z, t)$ is

$$\begin{cases} \frac{\partial f(x,y,z,t)}{\partial x} \approx \frac{f^n\left(i+\frac{1}{2},j,k\right)-f^n\left(i-\frac{1}{2},j,k\right)}{\Delta x} \\ \frac{\partial f(x,y,z,t)}{\partial y} \approx \frac{f^n\left(i,j+\frac{1}{2},k\right)-f^n\left(i,j-\frac{1}{2},k\right)}{\Delta y} \\ \frac{\partial f(x,y,z,t)}{\partial z} \approx \frac{f^n\left(i,j,k+\frac{1}{2}\right)-f^n\left(i,j,k-\frac{1}{2}\right)}{\Delta z} \\ \frac{\partial f(x,y,z,t)}{\partial t} \approx \frac{f^{n+1/2}(i,j,k)-f^{n+1/2}(i,j,k)}{\Delta t} \end{cases}. \quad (11)$$

Based on equations 6 and 11, we obtain

$$E_x^{n+1}\left(i+\frac{1}{2},j,k\right) = \frac{2\gamma-\overline{\sigma}\left(i+\frac{1}{2},j,k\right)\Delta t_n}{2\gamma+\overline{\sigma}\left(i+\frac{1}{2},j,k\right)\Delta t_n} E_x^n\left(i+\frac{1}{2},j,k\right) +$$

$$\frac{4\Delta t_n}{2\gamma+\overline{\sigma}\left(i+\frac{1}{2},j,k\right)\Delta t_n}\left[\frac{H_z^{n+1/2}\left(i+\frac{1}{2},j+\frac{1}{2},k\right)-H_z^{n+1/2}\left(i+\frac{1}{2},j-\frac{1}{2},k\right)}{\Delta y_{j-1}+\Delta y_j} - \frac{H_y^{n+1/2}\left(i+\frac{1}{2},j,k+\frac{1}{2}\right)-H_y^{n+1/2}\left(i+\frac{1}{2},j,k-\frac{1}{2}\right)}{\Delta z_{k-1}+\Delta z_k}\right], \quad (12)$$

where, $\overline{\sigma}\left(i+\frac{1}{2},j,k\right)$ is the averaged conductivities of the four cells connected by the magnetic loop:

$$\begin{cases} \overline{\sigma}\left(i+\frac{1}{2},j,k\right) = \omega_1\sigma(i,j-1,k-1)+\omega_2\sigma(i,j,k-1)+\omega_3\sigma(i,j-1,k)+\omega_4\sigma(i,j,k) \\ \omega_1 = \frac{\Delta y_{j-1}\Delta z_{k-1}}{(\Delta y_{j-1}+\Delta y_j)(\Delta z_{k-1}+\Delta z_k)} \\ \omega_2 = \frac{\Delta y_j\Delta z_{k-1}}{(\Delta y_{j-1}+\Delta y_j)(\Delta z_{k-1}+\Delta z_k)} \\ \omega_3 = \frac{\Delta y_{j-1}\Delta z_k}{(\Delta y_{j-1}+\Delta y_j)(\Delta z_{k-1}+\Delta z_k)} \\ \omega_4 = \frac{\Delta y_j\Delta z_k}{(\Delta y_{j-1}+\Delta y_j)(\Delta z_{k-1}+\Delta z_k)} \end{cases}. \quad (13)$$

Based on equations 7 and 11, we obtain

$$E_y^{n+1}\left(i,j+\frac{1}{2},k\right) = \frac{2\gamma-\overline{\sigma}\left(i,j+\frac{1}{2},k\right)\Delta t_n}{2\gamma+\overline{\sigma}\left(i,j+\frac{1}{2},k\right)\Delta t_n} E_y^n\left(i,j+\frac{1}{2},k\right) +$$

$$\frac{4\Delta t_n}{2\gamma+\overline{\sigma}\left(i,j+\frac{1}{2},k\right)\Delta t_n}\left[\frac{H_x^{n+1/2}\left(i,j+\frac{1}{2},k+\frac{1}{2}\right)-H_x^{n+1/2}\left(i,j+\frac{1}{2},k-\frac{1}{2}\right)}{\Delta z_{k-1}+\Delta z_k} - \frac{H_z^{n+1/2}\left(i+\frac{1}{2},j+\frac{1}{2},k\right)-H_z^{n+1/2}\left(i-\frac{1}{2},j+\frac{1}{2},k\right)}{\Delta x_{i-1}+\Delta x_i}\right], \quad (14)$$

where,

$$\begin{cases} \overline{\sigma}\left(i,j+\frac{1}{2},k\right) = \omega_1\sigma(i-1,j,k-1)+\omega_2\sigma(i,j,k-1)+\omega_3\sigma(i-1,j,k)+\omega_4\sigma(i,j,k) \\ \omega_1 = \frac{\Delta x_{i-1}\Delta z_{k-1}}{(\Delta x_{i-1}+\Delta x_i)(\Delta z_{k-1}+\Delta z_k)} \\ \omega_2 = \frac{\Delta x_i\Delta z_{k-1}}{(\Delta x_{i-1}+\Delta x_i)(\Delta z_{k-1}+\Delta z_k)} \\ \omega_3 = \frac{\Delta x_{i-1}\Delta z_k}{(\Delta x_{i-1}+\Delta x_i)(\Delta z_{k-1}+\Delta z_k)} \\ \omega_4 = \frac{\Delta x_i\Delta z_k}{(\Delta x_{i-1}+\Delta x_i)(\Delta z_{k-1}+\Delta z_k)} \end{cases}. \quad (15)$$

Based on equations 8 and 11, we obtain

$$E_z^{n+1}\left(i,j,k+\frac{1}{2}\right) = \frac{2\gamma-\overline{\sigma}\left(i,j,k+\frac{1}{2}\right)\Delta t_n}{2\gamma+\overline{\sigma}\left(i,j,k+\frac{1}{2}\right)\Delta t_n} E_z^n\left(i,j,k+\frac{1}{2}\right) +$$

$$\frac{4\Delta t_n}{2\gamma+\overline{\sigma}\left(i,j,k+\frac{1}{2}\right)\Delta t_n}\left[\frac{H_y^{n+1/2}\left(i+\frac{1}{2},j,k+\frac{1}{2}\right)-H_y^{n+1/2}\left(i-\frac{1}{2},j,k+\frac{1}{2}\right)}{\Delta x_{i-1}+\Delta x_i} - \frac{H_x^{n+1/2}\left(i,j+\frac{1}{2},k+\frac{1}{2}\right)-H_x^{n+1/2}\left(i,j+\frac{1}{2},k-\frac{1}{2}\right)}{\Delta y_{j-1}+\Delta y_j}\right], \quad (16)$$

Where,

$$\begin{cases} \overline{\sigma}\left(i,j,k+\frac{1}{2}\right) = \omega_1\sigma(i-1,j-1,k) + \omega_2\sigma(i,j-1,k) + \omega_3\sigma(i,j-1,k) + \omega_4\sigma(i,j,k) \\ \omega_1 = \frac{\Delta x_{i-1}\Delta y_{j-1}}{(\Delta x_{i-1}+\Delta x_i)(\Delta y_{j-1}+\Delta y_j)} \\ \omega_2 = \frac{\Delta x_i\Delta y_{j-1}}{(\Delta x_{i-1}+\Delta x_i)(\Delta y_{j-1}+\Delta y_j)} \\ \omega_3 = \frac{\Delta x_{i-1}\Delta y_j}{(\Delta x_{i-1}+\Delta x_i)(\Delta y_{j-1}+\Delta y_j)} \\ \omega_4 = \frac{\Delta x_i\Delta y_j}{(\Delta x_{i-1}+\Delta x_i)(\Delta y_{j-1}+\Delta y_j)} \end{cases} . \quad (17)$$

Based on equations 3 and 11, we obtain

$$H_x^{n+\frac{1}{2}}\left(i,j+\frac{1}{2},k+\frac{1}{2}\right) = H_x^{n-\frac{1}{2}}\left(i,j+\frac{1}{2},k+\frac{1}{2}\right) + \frac{\Delta t_{n-1}+\Delta t_n}{2\mu_0}\left[\frac{E_y^n\left(i,j+\frac{1}{2},k+1\right)-E_y^n\left(i,j+\frac{1}{2},k\right)}{\Delta z_k} - \frac{E_z^n\left(i,j+1,k+\frac{1}{2}\right)-E_z^n\left(i,j,k+\frac{1}{2}\right)}{\Delta y_j}\right]. \quad (18)$$

Based on equations 4 and 11, we obtain

$$H_y^{n+\frac{1}{2}}\left(i+\frac{1}{2},j,k+\frac{1}{2}\right) = H_y^{n-\frac{1}{2}}\left(i+\frac{1}{2},j,k+\frac{1}{2}\right) + \frac{\Delta t_{n-1}+\Delta t_n}{2\mu_0}\left[\frac{E_z^n\left(i+1,j,k+\frac{1}{2}\right)-E_z^n\left(i,j,k+\frac{1}{2}\right)}{\Delta x_i} - \frac{E_x^n\left(i+\frac{1}{2},j,k+1\right)-E_x^n\left(i+\frac{1}{2},j,k\right)}{\Delta z_k}\right]. \quad (19)$$

Based on equations 9 and 11, we obtain

$$H_z^{n+\frac{1}{2}}\left(i+\frac{1}{2},j+\frac{1}{2},k\right) = H_z^{n+\frac{1}{2}}\left(i+\frac{1}{2},j+\frac{1}{2},k+1\right) + \Delta z_k\left[\frac{H_x^{n+\frac{1}{2}}\left(i+1,j+\frac{1}{2},k+\frac{1}{2}\right)-H_x^{n+\frac{1}{2}}\left(i,j+\frac{1}{2},k+\frac{1}{2}\right)}{\Delta x_i} + \frac{H_y^{n+\frac{1}{2}}\left(i+\frac{1}{2},j+\frac{1}{2},k+\frac{1}{2}\right)-H_y^{n+\frac{1}{2}}\left(i+\frac{1}{2},j,k+\frac{1}{2}\right)}{\Delta y_i}\right]. \quad (20)$$

Typical transient electromagnetic equipment uses receiver loops for measuring the time derivative of the magnetic field. So $\partial B_z/\partial t$ is calculated at every time steps:

$$(\partial B_z/\partial t)\left(i+\frac{1}{2},j+\frac{1}{2},k\right) = \frac{E_x(i,j+1,k)-E_x(i,j,k)}{\Delta y_j} - \frac{E_y(i+1,j,k)-E_y(i,j,k)}{\Delta x_i}. \quad (21)$$

Stability

Following the Courant–Friedrichs–Lewy condition (Mitchel and Griffiths, 1980), we calculate the artificial dielectric constant using:

$$\gamma = \frac{4}{\mu_0}\left(\frac{\Delta t_n}{\Delta_{min}}\right)^2, \quad (22)$$

where Δ_{min} is the minimal grid size and Δt_n is the time step size.

The time step size is calculated as follows:

$$\Delta t_n = \alpha\Delta_{min}\sqrt{\mu_0\sigma_{air}t_n/6}, \quad (23)$$

where α is a constant (typically ranges from 0.4 to 0.8), σ_{air} is the conductivity of the air, and t_n is the advancing transient time. The air conductivity σ_{air} should be maximized to avoid small time step size. Commer et al. (2015) find that a contrast ranging from 1:100 to 1:500 is a

compromise between accuracy and computing effort for their models. Based on their results, a contrast of 1:300 is used in the following examples.

Initial conditions

At a time after the current is switched off, the electromagnetic field excited by a vertical magnetic dipole source in homogeneous whole-space medium are as follows:

$$\begin{cases} H_x(x,y,z) = \frac{Mzx}{4\pi r^5}\left[3\phi(u) - \sqrt{2/\pi}u(3+u^2)e^{-(u^2/2)}\right] \\ H_y(x,y,z) = \frac{Mzy}{4\pi r^5}\left[3\phi(u) - \sqrt{2/\pi}u(3+u^2)e^{-(u^2/2)}\right] \\ H_z(x,y,z) = \frac{M}{4\pi r^5}\left\{\left(2z^2 - \sqrt{x^2+y^2}\right)\phi(u) - \sqrt{2/\pi}\left[2z^2 - \sqrt{x^2+y^2}(1+u^2)\right]e^{-(u^2/2)}\right\} \\ E_x(x,y,z) = \sqrt{2/\pi}\frac{Myu^5}{4\pi r^5\sigma}e^{-(u^2/2)} \\ E_y(x,y,z) = \sqrt{2/\pi}\frac{Mxu^5}{4\pi r^5\sigma}e^{-(u^2/2)} \\ E_z(x,y,z) = 0 \end{cases}, \quad (25)$$

where (x,y,z) is the spatial position, $r = \sqrt{x^2+y^2+z^2}$, M is the magnetic moment, $\phi(u) = \sqrt{2/\pi}\int_0^u e^{-(u^2/2)}dt$ is the probability integral, $u = 2\pi r\sqrt{\sigma}/\sqrt{2\pi t \times 10^7}$, t is the time, and σ is the conductivity of the homogeneous whole-space medium.

We calculate the initial field using above equations. In the ground detection, the air conductivity above the transmitter loop and the earth conductivity below the transmitter loop are significantly different. Therefore, the initial field is an approximate initial field. We didn't find significant effect on the modelling by using different model for the initial field, that is, the approximate initial field can be calculated using a conductivity independent of the model.

To achieve modeling for large transmitter loop configurations, we divide the transmitter loop into multiple superimposed magnetic dipole sources as shown in Figure 2. A total of 64 superimposed whole-space magnetic dipole sources are used in the following examples.

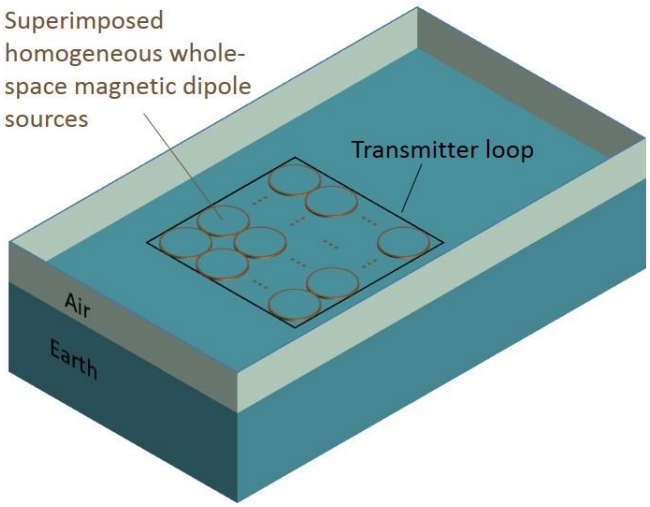

Figure 2. Large transmitter loop is divided into multiple superimposed whole-space magnetic dipole sources.

We calculate the initial electric field at an initial time similar to that presented by Wang and Hohmann (1993) as follows:

$$t_{0E} = 1.13\mu_0\sigma_{air}\Delta_{min}^2. \quad (26)$$

We calculate the initial magnetic field at an initial time:

$$t_{0H} = t_{0E} + 1/2\Delta t_0, \tag{27}$$

where,

$$\Delta t_0 = \alpha\Delta_{min}\sqrt{\mu\sigma_{air}t_{0E}/6}. \tag{28}$$

Boundary conditions

For the outer boundaries, we set the tangential electric field to zero to satisfy a homogeneous Dirichlet boundary condition. For the air–earth interfaces, we include the air into the FD grids and one does not need to define additional boundary conditions, which facilitates the simulation of the non-flat topography model.

EXAMPLES

Conductive brick in a half-space

As shown in Figure 7a, in a homogeneous half space with conductivity of 0.1 S/m, a conductivity brick of 2 S/m is located at the depth of 30 m, with size of 100 m×40 m×30 m in the x-, y-, and z-directions, respectively. A central-loop configuration is adopted, and the loop size is 100 m×100 m.

For this example, the model size is 5140 m×5135 m×7530 m, and it contains 17×18×18 grid cells. In the x direction, the grid size of the 5 grid cells in the center is 20 m, which grows outward with a growth factor of two. In the y direction, the grid size is 10 m at the receiver and 20 m at the conductive brick, which grows outward with a growth factor of two. In the z direction, the grid size of the six grid cells near the earth–air interface and conductive brick is 15 m, which grows upward with a growth factor of two and downward with a growth factor of three. Figure 7b shows the mesh for the section in Figure 7a.

Figure 8 shows the numerical solutions as calculated by the FE method of Li et al. (2017) and the method presented here. The two solutions are in good agreement with each other. For this example, the total number of time steps is 2400, and the run-time is 0.48 s.

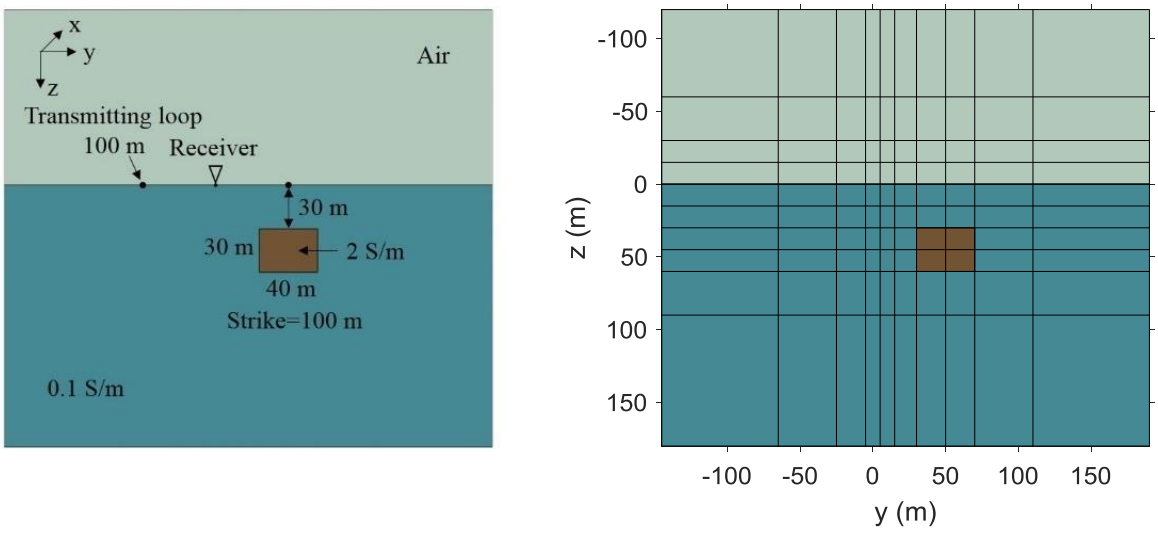

(a) (b)

Figure 7. Model of a conductive brick in a half-space.

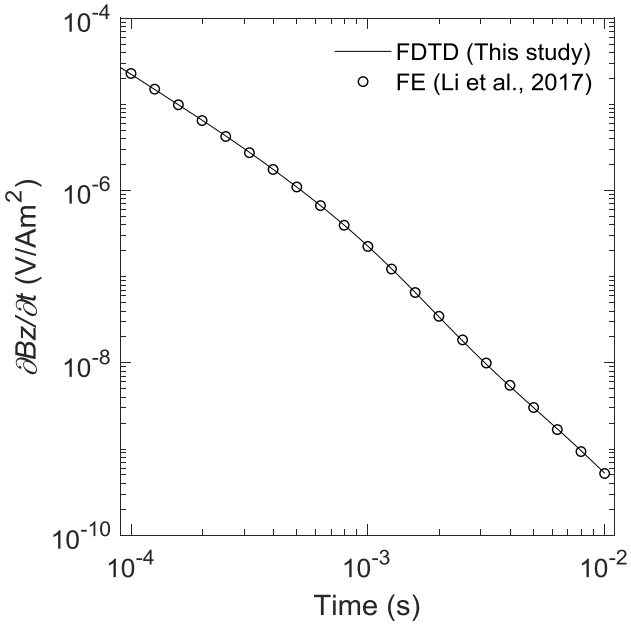

Figure 8. Numerical results.

Complex conductor at a vertical contact

As shown in Figure 10a, the underground 0–50 m is a thin 0.1 S/m conductive layer, below which the earth is divided into two parts (0.01 and 0.0033333 S/m) by a vertical contact. At the contact, a 1 S/m conductive anomaly, which is approximately 400 m long, 100 m wide, and 500 m in depth extent, is located within the right part. The loop size is still 100 m×100 m, and its center is located at (0, 50, 0) m. The receivers are located at (0, 50, 0), (0, 150 ,0), (0, 450, 0), and (0, 1050, 0) m.

For this example, the model size is 51,400 m×36,810 m×51,700 m, and this model contains 30×53×39 grid cells. Figure 10b shows the mesh for the section in Figure 10a. In the x direction, the minimum grid size is 10 m, which grows outward with growth factors of 1.5–2. In the y direction, the minimum grid size is 10 m at the receivers, which grows outward with a growth factor of two. In the z direction, the minimum grid size is 12.5 m near the earth–air interface and the anomaly edge, which grows with a growth factor of two.

Figure 11 shows the numerical results as calculated by the FE method of Li et al. (2017) and the method presented here. A good agreement for both solutions is observed. The total number of time steps is 6985, and the run-time is 9.72 s.

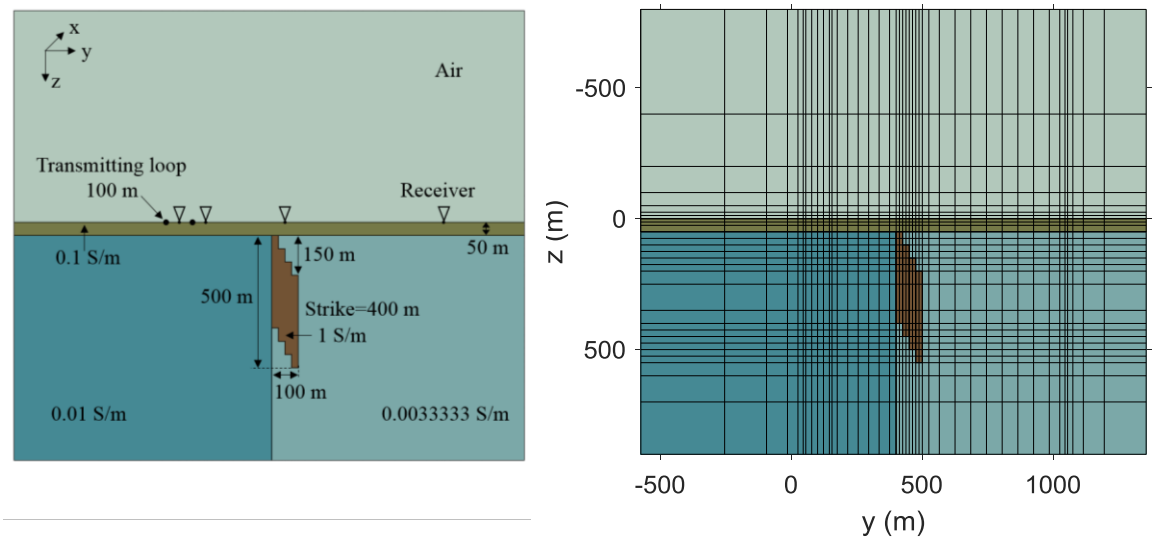

(a) (b)

Figure 10. Model of a complex conductor at a vertical contact.

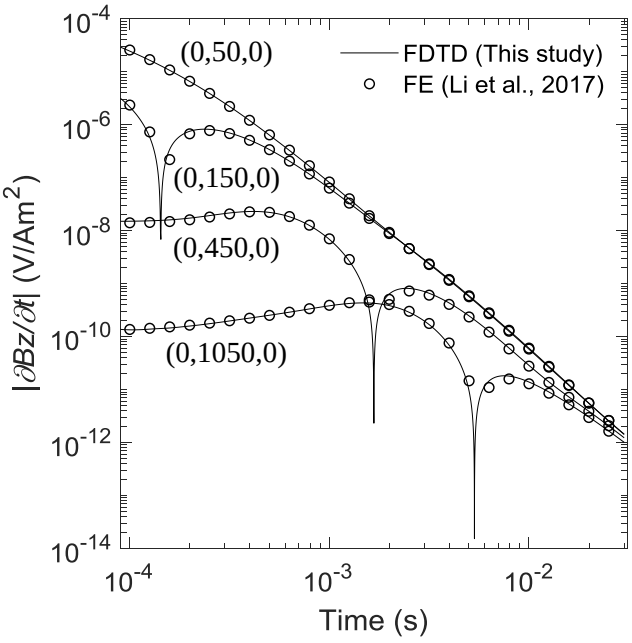

Figure 11. Numerical results.

Full paper:

LiFei and JiulongCheng, 2023, 3D finite-difference transient electromagnetic modeling with a whole-space initial field, Geophysics, online: https://doi.org/10.1190/geo2021-0828.1.